# Video-Guided Real-to-Virtual Parameter Transfer for Viscous Fluids – Supplementary Material

TETSUYA TAKAHASHI, University of North Carolina at Chapel Hill
MING C. LIN, University of Maryland at College Park, University of North Carolina at Chapel Hill

CCS Concepts: • **Computing methodologies → Physically-based simulation**; **Material parameter optimization**.

**ACM Reference Format:**
Tetsuya Takahashi and Ming C. Lin. 2019. Video-Guided Real-to-Virtual Parameter Transfer for Viscous Fluids – Supplementary Material. *ACM Trans. Graph.* 38, 6, Article 237 (November 2019), 3 pages. https://doi.org/10.1145/3355089.3356551

## 1 VISCOSITY PARAMETER IDENTIFICATION WITH PIV

In this supplementary material, we describe the viscosity parameter identification with particle image velocimetry (PIV) data for viscous fluids captured from real-world experiments. In the experiments, we use a simple setup, where a solid ball falls inside of viscous fluids, to capture the velocity fields with PIV because of the ease of the experiments in the same condition without a special setup. Although it is possible to identify viscosity parameters with a simpler way, e.g., by matching the velocity of the solid ball with a simulated solid ball, in this scenario, we note that the simple approach is not applicable if the solid ball is moved in a prescribed manner while PIV data can still be used for parameter identification, and thus can be considered as more general. In this report, we explain the parameter identification with PIV data and provide some experimental results as an extra validation for our general parameter identification framework.

The algorithm of our framework with PIV data is essentially same as the one for example videos, and our goal is to identify viscosity parameters with which our viscous fluid simulator generates fluid flows as close as possible to the PIV data. Similar to the case of example videos, our framework first captures velocity fields using PIV from real world fluid phenomena, and preprocesses the captured data to make them amenable for the optimization. Then, we perform iterative optimization with forward viscous fluid simulations and finally output identified viscosity parameters. In the following, we describe major processes for PIV data, i.e., objective function formulation §1.1, velocity field capture §1.2, preprocess §1.3, and objective function evaluation §1.4. The iterative optimization can be performed in the same way as for the identification with example videos.

Authors' addresses: Tetsuya Takahashi, Computer Science, University of North Carolina at Chapel Hill, tetsuya@cs.unc.edu; Ming C. Lin, Computer Science, University of Maryland at College Park, University of North Carolina at Chapel Hill, lin@cs.umd.edu.


0730-0301/2019/11-ART237 $15.00
https://doi.org/10.1145/3355089.3356551

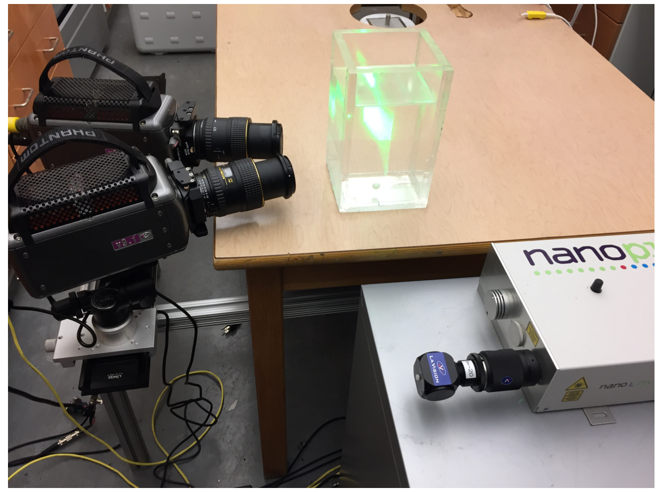


Fig. 1. Our PIV setup to capture velocity fields. Laser is injected into viscous fluids to capture the 2D velocity fields on the sheet.

### 1.1 Objective Function

PIV is an optical method for directly capturing the velocity fields of fluid flows in the real world, and is widely used in the scientific fields for validation purposes. While there are various types of PIV setup and related algorithm, e.g., to capture 3D velocity fields [Xiong et al. 2017], one commonly available PIV system captures 2D velocity fields on a laser sheet injected by the system, as shown in Figure 1.

Since PIV can directly measure the fluid velocities from real fluid flows, we formulate our objective function as

$$E = \frac{1}{M} \sum_{f=0}^{N-1} \|\mathbf{C}_f^{\frac{1}{2}}(\tilde{\mathbf{u}}_f - \hat{\mathbf{u}}_f)\|_2^2, \tag{1}$$

where $M$ denotes the number of velocity samples used in the optimization, $f$ index for frames, $N$ total count of frames considered in the optimization, $\mathbf{C}$ a diagonal coefficient matrix, $\tilde{\mathbf{u}}$ the 2-dimensional interpolated fluid velocities from the simulation, and $\hat{\mathbf{u}}$ the 2-dimensional fluid velocities captured with PIV.

### 1.2 Capturing Velocity Fields

To capture the velocity fields using PIV, we setup an experimental setting, as shown in Figure 1. In our setting, we first prepare a container filled with viscous fluids, two calibrated and synchronized cameras positioned next to each other, and a laser device to inject thin sheet-shaped laser into the viscous fluids. Then, we put tiny metal particles into the viscous fluids so that these particles reflect the injected laser, and the cameras can capture the movement and

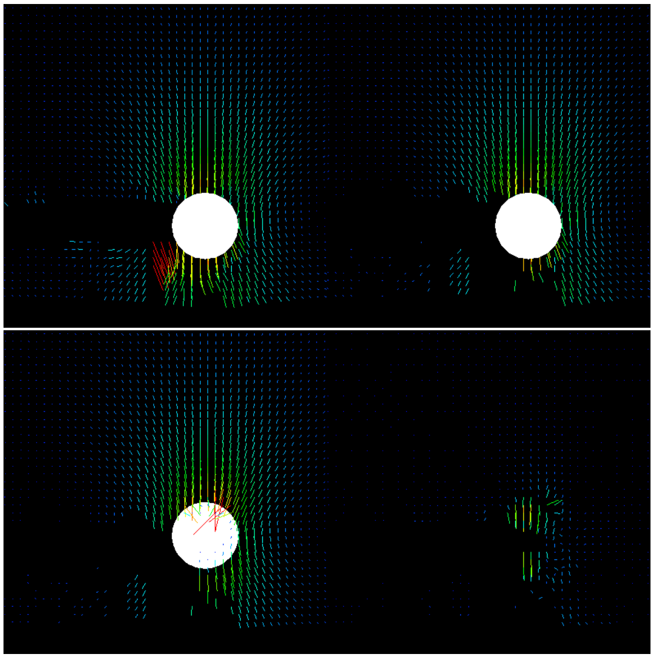

Fig. 2. Velocity field illustration. White sphere represents the solid ball falling inside the viscous fluids. (Top left) velocity fields captured with PIV. (Top right) valid velocity fields. (Bottom left) velocity fields interpolated from velocity fields generated with our solver. (Bottom right) Velocity field differences between the valid velocity fields and the interpolated velocity fields.

velocities of these particles using optical flow algorithms. The resulting velocity fields computed with PIV are uniformly aligned and within a small window on the 2D (xy) plane produced by the injected laser.

To induce fluid velocities, we chose a simple scenario, where a solid ball falls down inside of the viscous fluids, so that one can easily and consistently regenerate a similar setup (see Figure 3 (left)). We carefully put the solid ball such that the center of the solid ball is exactly on the sheet created by the laser device not to induce out of plane velocities (i.e., z-component of fluid velocities equals 0), and then measure velocity fields perturbed due to the falling solid ball. One example of the 2D velocity fields captured with PIV is shown in Figure 2 (top left).

## 1.3 Preprocessing

While the velocity fields taken with PIV can sufficiently capture an overall flow of viscous fluids, there are some inconsistency due to the noise, which can be interpreted as unnatural, sudden velocity changes. Thus, we aim to remove the inconsistency from the captured velocity fields to make them temporally consistent and amenable in the optimization step.

Since the captured velocity fields are taken from the real fluid flows, their behaviors should follow the Newton's law, and thus the velocity fields should be sufficiently smooth in the temporal direction. Thus, we first measure the smoothness of the captured velocity fields with the Laplacian on the temporal direction:

$$\nabla_f^2 \hat{\mathbf{u}} = \frac{\hat{\mathbf{u}}_{f+1} - 2\hat{\mathbf{u}}_f + \hat{\mathbf{u}}_{f-1}}{\Delta t^2}. \tag{2}$$

Then, we evaluate the validity of the captured velocities by comparing the magnitude of the Laplacian $\|\nabla_f^2 \hat{\mathbf{u}}\|$ with the norm of the measured velocity itself $\|\hat{\mathbf{u}}\|$, and treat velocity fields as valid if $\|\nabla_f^2 \hat{\mathbf{u}}\| < \alpha \|\hat{\mathbf{u}}\|$, where $\alpha$ denotes a threshold parameter to adjust the necessary smoothness to be valid. In practice, we eliminate invalid velocities by setting coefficients in the objective function as

$$c_f = \begin{cases} 1 & \text{if } \|\nabla_f^2 \hat{\mathbf{u}}\| < \alpha \|\hat{\mathbf{u}}\| \\ 0 & \text{otherwise} \end{cases} \tag{3}$$

where $c$ denotes a diagonal entry of the coefficient matrix. It is worth noting that although non-binary coefficients could be used, we found that binary coefficients are generally preferable because the binary coefficients can completely eliminate the noisy velocity fields, and in general there are sufficient numbers of valid velocity fields to be used as a reference. Figure 2 (top right) illustrates only valid velocity fields.

## 1.4 Evaluating Objective Function

To evaluate the objective function, it is necessary to perform the fluid simulation. For the simulation setup, we measure the size of the container and solid ball and density of the ball. Then, we manually estimate positions of the ball and compute solid velocities from the positions using finite difference. During the simulation, we interpolate the fluid velocities at the positions, where valid velocities are defined (see Figure 2 (bottom left)). Since the velocity fields from the fluid simulation are available over the entire simulation domain (unlike PIV velocity fields), we can straightforwardly interpolate the velocities and compute the objective function. The difference between the valid PIV data and the interpolated velocities is illustrated in Figure 2 (bottom right). We note that since fluid velocities are extrapolated into the solid ball, the computation of the objective function is valid even if the positions of the solid ball deviate from those in the example data.

In our framework, velocity fields obtained from PIV are available only within a small window on the 2D sheet. As such, it is not possible to replace the PIV velocity fields as initial or intermediate velocity fields for each step of the forward simulation. Consequently, it is necessary to rely on the simulation results at each frame, which would deviate from the example data due to the accumulated errors over multiple steps. However, we minimize the velocity deviations from the example data over multiple frames as a space-time optimization problem, and thus the resulting viscosity parameters are considered as optimal over the given time span although different parameters would generate smaller velocity deviations from the example data for a specific short term.

# 2 VALIDATION RESULTS

We implemented our framework with C++, and used a viscous fluid solver based on [Batty and Bridson 2008; Takahashi and Lin 2019] Our experiments are executed on a Linux machine with 24-core 2.50GHz Intel Xeon and 256 GB RAMs. For the parameter

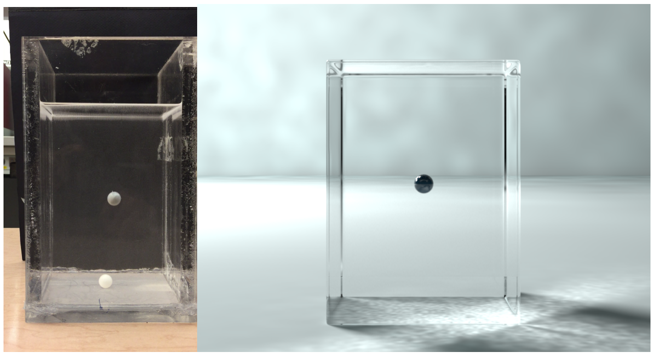

Fig. 3. A sphere falling inside of viscous fluids. (Left) experimental setup for capturing PIV velocity fields. (Right) our simulation results with the identified viscosity parameter. The falling behavior of the simulated ball is in good agreement with the falling ball in the real world used to capture PIV data.

Table 1. Viscosity parameter identification results with PIV velocity fields. $\rho_f$ denotes fluid density ($kg/m^3$), $\hat{\eta}$ fluid viscosity ($kg/(s \cdot m)$), $r$ solid ball radius $1.0 \times 10^{-3}(m)$, $\rho_s$ solid ball density ($kg/m^3$), $u_\infty$ the terminal velocity of the solid ball ($m/s$), $Re$ Reynolds number, $\eta$ identified viscosity value ($kg/(s \cdot m)$), and $\epsilon$ relative error (%). In general, relative errors are small.

| Name | $\rho_f$ | $\hat{\eta}$ | $r$ | $\rho_s$ | $u_\infty$ | $Re$ | $\eta$ | $\epsilon$ |
|---|---|---|---|---|---|---|---|---|
| plastic | 970.79 | 1.03 | 6.25 | 1555.00 | -0.04 | 0.47 | 0.96 | 6.80 |
| steel | 970.79 | 1.03 | 4.76 | 8050.00 | -0.12 | 1.07 | 1.12 | 8.73 |

identification, we typically formulate the objective function with up to 50 frames to make the space-time optimization manageable.

## 2.1 PIV Velocity Fields

To validate our framework, we use a simple experimental setting, where a solid ball is falling inside of viscous fluids. This experimental setting is shown in Figure 3 (left). We capture velocity fields with this setup, and used the captured velocity fields as input for our framework. In this experiment, we use silicone oils as viscous fluids and measured their viscosity values with a viscometer for comparison. We use different types of balls: "plastic" and "steel". Because of different size and density of the balls, the falling speed of the balls are also different leading to distinct fluid flow patterns (i.e., different Reynolds numbers). The parameters and results are summarized in Table 1. We note that in the scenes "plastic" and "steel", Stokes' law is not valid since Reynolds number is not sufficiently low ($Re \ll 1$), and thus it is not possible to identify viscosity parameters based on the Stokes' law. In this experiment, for the identification results of "plastic" and "steel", the relative errors are small and is within 10%.

For the demonstration of the parameter identification result, we simulate the falling sphere scenario, where we captured the PIV velocity fields. The result is given in Figure 3 (right) and in the accompanying video. The resulting movement of the simulated solid ball is in good agreement with the ball in the real world counterpart.

## REFERENCES

Christopher Batty and Robert Bridson. 2008. Accurate Viscous Free Surfaces for Buckling, Coiling, and Rotating Liquids. In *Proceedings of the 2008 ACM SIGGRAPH/Eurographics Symposium on Computer Animation*. 219–228.

Tetsuya Takahashi and Ming C. Lin. 2019. A Geometrically Consistent Viscous Fluid Solver with Two-Way Fluid-Solid Coupling. *Computer Graphics Forum* 38, 2 (2019), 49–58.

Jinhui Xiong, Ramzi Idoughi, Andres A. Aguirre-Pablo, Abdulrahman B. Aljedaani, Xiong Dun, Qiang Fu, Sigurdur T. Thoroddsen, and Wolfgang Heidrich. 2017. Rainbow Particle Imaging Velocimetry for Dense 3D Fluid Velocity Imaging. *ACM Trans. Graph.* 36, 4, Article 36 (July 2017), 14 pages.